SATELLITE DERIVED BATHYMETRY FOR DETECTING CHANGES IN LIGHTHOUSE CREEK'S UNDERWATER TOPOGRAPHY

Dupe N. Olayinka and Chukwuma J. Okolie

Department of Surveying & Geoinformatics, Faculty of Engineering,
University of Lagos, Lagos State, Nigeria.
Correspondence: nihinolayinka@yahoo.co.uk, mrjohnokolie@gmail.com,
dsaka@unilag.edu.ng

Abstract
Rivers exhibit tremendous spatio-temporal variability because of variations in streamflow and sediment input. Satellite bathymetry provides a viable method for monitoring these changes in riverbed topography and provides data from which morphological parameters are estimated. This study applied a linear ratio model on Landsat imagery to produce bathymetric maps for the shallow Lighthouse Creek at three epochs (2002, 2006 and 2015). The final bathymetry was obtained by applying tidal corrections to the image-derived bathymetry. The time-series bathymetries were compared to detect changes in the creek's underwater terrain. Results show a decrease of 2,102,390.5m^3 in the creek's surface volume from 2002 – 2006 and an increase of 224,920m^3 from 2006 – 2015. To model depth change over time, a navigation route was designed along the creek's length and depth values were plotted against distances drawn along the longitudinal profile. The results show an indication of increasing accretion in the Lighthouse Creek until the 2006 time period when the seabed material started eroding gradually from the Creek. The study recommends further investigation into the source of the initial sediment build-up and the direction of the present sediment outflow.

Keywords: Bathymetry, Satellite-Derived Bathymetry, Echo-Sounding, Landsat, Linear-ratio model, Lighthouse Creek

1.0 Introduction

Rivers exhibit tremendous variability across space and time because of variations in streamflow and sediment input (Lea and Legleiter, 2015). Monitoring the changes in riverbed topography may be particularly important because they provide data from which morphological parameters are estimated. Also, seabed morphology can change rapidly in response to storm surges, sea level rise, changes in river conditions, and engineering activity such as dredging. Dense and accurate topographical data acquired through time is needed to develop understanding and to assess the impact of earth surface processes. The traditional definition of elevation is considered the above water measurement of topographical features, but in order to enhance the knowledge of global environmental factors, underwater elevation or depth (bathymetry) must be measured as well (Rodriguez, 2015).

Bathymetry is the science of determining the topography or shape of the rivers, lakes, seas, or the ocean floor (Herban and Alionescu, 2012). It is the underwater equivalent to hypsometry or

topography. In the oceans, sea floor topography refers to the geographic features of the sea floor including the configuration of a surface and the position of its natural and man-made features; and detailed nautical charts are fundamental for many sciences such as physical oceanography, biology and marine geology (Zirek and Sunar, 2014). The importance of having accurate bathymetry estimations is evident from a variety of scientific fields related with monitoring, evaluation and assessment of marine environments. Nowadays bathymetric information is of fundamental importance in coastal and marine planning and management, nautical navigation, and scientific studies of marine environments and from the economical perspective of using natural resources on the coast *(Herban and Alionescu, 2012)*.

Underwater elevation measurements historically used line measurements to obtain depth values (Rodriguez, 2015). Many shallow water areas are not accessible by hydrographic ships due to rocks, coral reefs or simply the shallowness of the water. Whilst they can be highly accurate, conventional bathymetric mapping from vessel-based echo-sounders are typically constrained by limited ground coverage, difficulties in accessing shallow coastal water and high operating cost. *S*atellite-derived bathymetry (SDB) provides a viable option for mapping the water column depth using imagery collected from space-borne satellites. Since imagery is typically densely packed with information in every pixel, SDB effectively provides a continuous 3D model of seafloor topography. Bathymetric mapping from optical remotely sensed images offers a more flexible, efficient and cost-effective means of mapping the water depth over broad areas (Gao, 2009). Remote Sensing systems are increasingly being utilized for such mapping. The sensors used to obtain the measurements of elevation or depth can vary, but are generally standardized. Active or passive remote sensing from aircraft and/or satellites could be the tools to solve the problem (Clark et al., 1987; Bierwirth et al., 1993; Liceaga-Correa et al., 2002; Vahtmäe et al., 2007 cited in Gholamalifard et al., 2013). However, the airborne systems and high resolution satellite data may not be easily accessible due to cost constraints, therefore freely available Landsat data were used for this study.

1.1 Model for Bathymetry Determination

The fundamental principle behind using remote sensing to map bathymetry is that different wavelengths of light will penetrate water to varying degrees. Intensity of the sun light I_d will be attenuated by interaction with the water column when passing through water length p as follows (Nga et al., 2007):

$$I_d = I_0 e^{-pk} \quad (1)$$

Where I_0 – intensity of the incident light and k – attenuation coefficient (Green et al., 2000).

Taking natural logarithms, Eq (1) becomes linear as follows:

$$log_e(I_d) = log_e(I_0) - pk \quad (2)$$

Different image bands react differently to attenuation. Red light attenuates rapidly in water and does not penetrate further than about 5m in clear water. On the contrary, blue light penetrates much further. The level of turbidity of the water is also another determining factor of the penetration depth. Suspended sediment particles,

phytoplankton and dissolved organic compounds will all affect the depth of penetration (and so limit the range over which optical data may be used to estimate depth) because they scatter and absorb light, thus increasing attenuation. Also, the coefficient of attenuation **k is dependent on the** wavelength. Longer wavelength light has a higher attenuation coefficient than short wavelengths. Therefore, red light is removed from white light passing vertically through water faster than blue. However not all wavelengths will have been attenuated to the same extent - there will still be shorter wavelength light at this depth. The reflectance of the water, R_w, which includes the bottom where the water is optically shallow, is defined as (Stumpf et al., 2003):

$$R_w = \frac{\pi L_w(\lambda)}{E_d(\lambda)} \quad (3)$$

where L_w is the water-leaving radiance, E_d is the downwelling irradiance entering the water, and is the spectral band. L_w and R_w refer to values above the water surface. R_w is found by correcting the total reflectance R_T for the aerosol and surface reflectance, as estimated by the near-IR band, and for the Rayleigh reflectance R_r. R_w is as given in Eq (4).

$$R_w = R_T(\lambda_i) - Y(\lambda_j)R_T(\lambda_{IR}) - R_T(\lambda_i) \quad (4)$$

Y is the constant to correct for spectral variation (equivalent to the Angstrom exponent in Gordon et al., (1983), subscript i denotes a visible channel, and subscript IR denotes the near-IR channel. R_T is found from Eq (5) given as:

$$R_T(\lambda_i) = \frac{\pi L_t(\lambda_i)/E_0(\lambda_i)}{\left(\frac{1}{r^2}\right) T_0(\lambda_i)T_1(\lambda_i)\cos\theta_0} \quad (5)$$

L_t is the (total) radiance measured at the satellite, E_0 is the solar constant, r is the earth–sun distance in astronomical units, θ_0 is the solar zenith angle, and T_0 and T_1 are the transmission coefficients for sun-to-earth and earth-to-satellite, respectively. Lyzenga (1985) devolved a linear technique to determine the water depth. The technique utilized a single band to define the relationship between the reflected radiance and water depth in cases where the optical properties of the water reflectance and the bottom reflectance are constant (Alsubaie, 2012). However, this method was limited in that it was unable to accurately model variable bottom types with various albedos. It therefore proved inaccurate for calculating water depth since the bottom albedos varied significantly (Green et al., 2000). These limitations inspired Stumpf et al., (2003) to develop an alternative model for transforming the reflectance in an attempt to determine the depth.

The principle behind Stumpf's ratio algorithm is the absorption degrees of different bands with different wavelengths where each band attenuates at a different degree while the energy penetrated the water. Thus, the band with the higher absorption degree decreases consistently faster while the depth increases. As the ratio increases so does the depth increase.

Stumpf et al., (2003) went further to remove the effects of varying albedo where both bands have a similar effect. The ratio between these bands was affected by the increase in depth more than the varying bottom albedo. As shown in Equation 6, this algorithm requires only two tunable parameters that could be computed using the linear regression method between the ratio result and ground truth (Alsubaie, 2012).

The ratio algorithm was compared with a standard linear transform using IKONOS satellite imagery as opposed to LIDAR bathymetry. The coefficients (m_1,m_0) were tuned manually to a few depths from a nautical chart in order to compute the ratio algorithm. Lyzenga's linear algorithm was tuned using multiple linear regressions against the LIDAR data. Results showed that both algorithms are equivalent over variable bottom type albedo and retrieve bathymetry in water depths less than 10–15m. However, while the linear transform does not distinguish depths greater than 15m, ratio transforms can also be applied to low-albedo water. Stumpf et al., (2003) thereafter posited that this method was robust and works well over variable bottom types. It also accounts better for water turbidity:

$$Z = m_1 \frac{\ln\left(nR_w(\lambda_i)\right)}{\ln\left(nR_w(\lambda_j)\right)} - m_0 \qquad (6)$$

Where m_1 ***(gain)*** is a tunable constant to scale the ratio to depth, n is a fixed constant for all areas to assume that the algorithm is positive, and m_0 is the offset for a depth of 0m where ($Z = 0$). R_w is the reflectance of water, and($\lambda_{i,j}$)are two different bands. The fixed value of n in Eq. 6 is chosen to assure both that the logarithm will be positive under any condition and that the ratio will produce a linear response with depth.

Studies have shown the satisfactory performance and robustness of the ratio algorithm (e.g. Peeri et al., 2012; Pennucci et al., 2006). In a synoptic review on models and methods for deriving bathymetry information using Remote Sensing technologies, Jawak et al., (2015) concluded that Stump's ratio model is robust in non-homogeneous environments and performs better in scattering turbidity than Lyzenga's linear band model. However, the ratio model is found to be somewhat noisier and cannot always adequately resolve fine morphology in water depths less than 15 - 20m. Also, Stumpf's algorithm may prove completely ineffective in waters where turbidity is the predominant factor defining attenuation in the water column. For better results, ground reference or in-situ datasets should be considered to represent a wide range of variance in bottom type and water column properties with statistically significant sample sizes at different depths.

These studies have demonstrated the satisfactory performance of Stumpf's model in variable bottom types. In a more recent effort, Olayinka and Okolie (2016) tested the accuracy of the ratio algorithm in determining bathymetry from a time series of Landsat imagery covering the present area under study (Lighthouse Creek, Lagos). The Landsat-derived depths were compared with in-situ depths from echo sounding. After the removal of outlier estimates, the standard errors in the estimated depths when compared with the sounded depths were 0.29m for year 2002, 0.31m for year 2006 and 0.27m for year 2015. The absolute differences between the actual depths and estimated depths at these

points ranged from 0.1 – 0.49m.

This study goes a step further by extending the application scope of the Landsat derived bathymetry in monitoring the dynamic nature of the creek's bottom over a 13-year time period (2002 – 2015).

2.0 Materials and Methods

This study explores the utility of the Landsat-derived bathymetry for monitoring changes in the underwater topography of the Lighthouse Creek. A time series of bathymetry at three epochs was generated using Landsat imagery from which changes in the seabed profile were quantitatively analysed.

2.1 Study Area

Lighthouse Creek is at the west of the Commodore Channel in the vicinity of Lagos Harbour just by the entrance to Badagry Creek in Lagos state, South-Western Nigeria. It lies beside the West Mole Wharf and the Atlas Cove Oil Terminal. Its geographic extent spans between longitudes 3

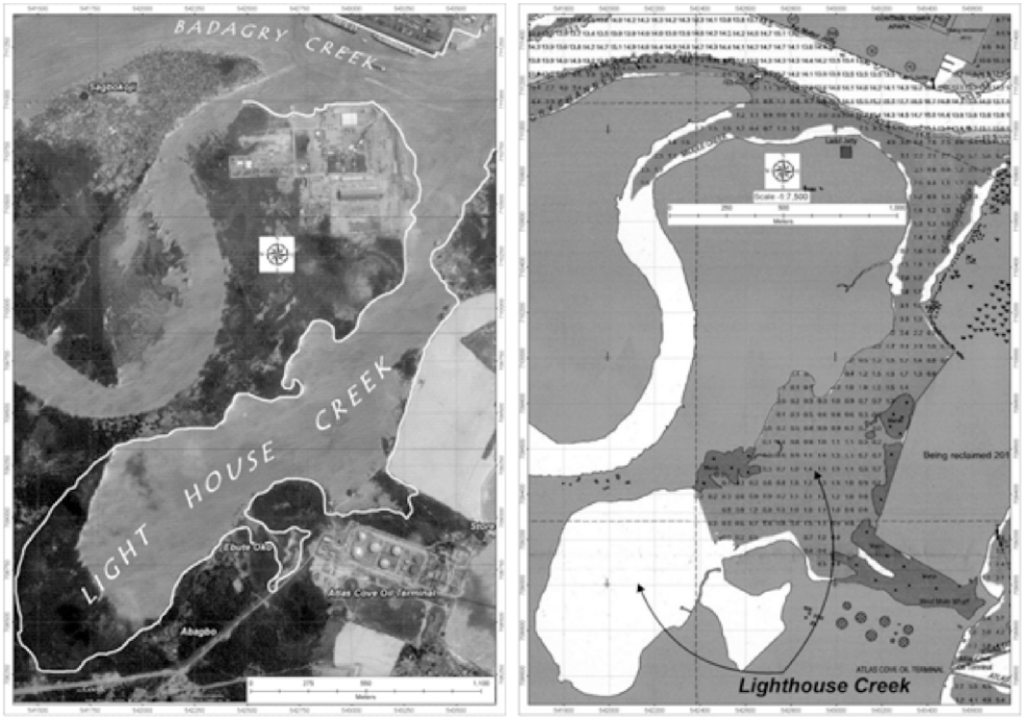

Figure 1: (a) Satellite image map of Lighthouse Creek (b) Chart showing extent of bathymetric coverage for Lighthouse Creek

Table 1: List of Datasets Used

Data	Publisher/ Source	Year
Hydrographic Chart (for reconnaissance)	Lagos Channel Management (LCM)	2014
Landsat Imageries	US Geological Surveys (USGS)	2002, 2006, 2015
Tidal Predictions	Nigerian Navy Hydrographic Office (NNHO)	2002, 2006, 2015

Table 2: Landsat Datasets

Landsat Data	Path/Row (WRS-2)	Acquisition Date (DD-MM-YYYY)	Acquisition Time (GMT +1)
Landsat 7 ETM+	191/55	28-12-02	10:51:17
		07-12-06	10:53:04
Landsat 8 OLI	191/55	06-01-15	11:02:59

2.3 Depth Estimation from Landsat Imagery

The methodology workflow is as shown in Figure 2. The spectral information of the Blue, Green and Near Infrared (NIR) bands were considered significant for this process. It was not necessary to convert the Landsat 8 pixel values to surface reflectance as the former could be used directly. First, threshold values at the land/water boundary (shown as profile graphs in Figures 3 – 5 representing the three epochs – 2002, 2006 and 2015 respectively) were used to separate water from the land. In the profile graphs, the smooth sections with low values represent water, whereas the fluctuation high value areas represent land. Most of the cloud cover was removed in this phase. Next, a low-pass preset focal filter was performed to smoothen the rasters and reduce the significance of anomalous cells. No-Data values were assigned to cells with values higher than the previously calculated water threshold value. The practical approach put forward by Hedley et al., (2005) was used to implement correction for sun glint and cloud cover that is a serious confounding factor for remote sensing in shallow water areas. The step was used to correct radiometric contribu-tion from low altitude clouds and glint from the Blue and Green bands. To do this, a narrow polygon was created over the NIR layer to cover the dark areas in the water. This polygon constituted a mask layer. The cells of the Blue, Green and NIR bands corresponding to the areas defined by the mask were extracted. Next, two sets of scatter plots were created for each image (Blue vs NIR and Green vs NIR). The slope of the trend line for the blue and green layers was calculated and inputted into the Hedley et al., (2005) algorithm.

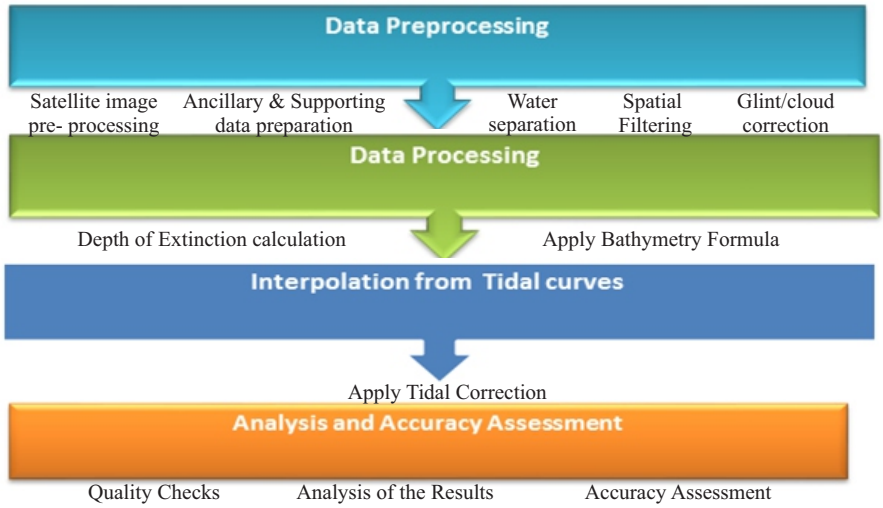

The readings from the tide prediction tables coinciding with the Landsat acquisition dates were plotted in Matlab and connected by a shape preserving interpolant. The Landsat scene centre times in Greenwich Mean Time (GMT) were converted to GMT + 1 by the addition of 1hr. The corresponding tide heights at the set time were then interpolated from the graphs. Next, the optic depth limit for inferring bathymetry (the extinction depth) was determined to be

The gain (m_1) and offset (m_0) for referencing the algorithm to the chart datum were determined through vertical referencing. In a final step, the bathymetry was calculated using the ratio algorithm. The final bathymetry was obtained after corrections gotten from tidal prediction values connected by a shape preserving interpolant were applied. All datasets were referenced to WGS84 datum Zone 31N.

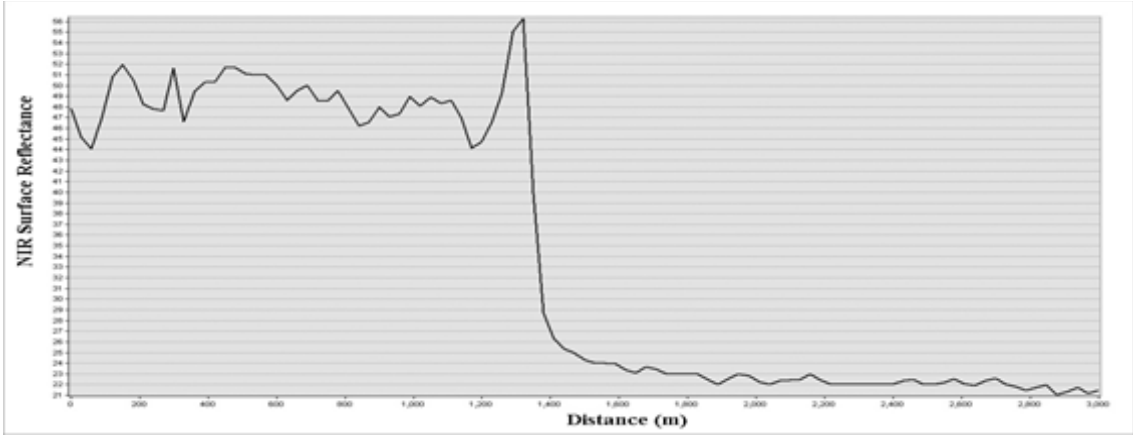

Figure 3: Profile graph for ***Landsat 7 NIR Band 4 – 2002 (Path/Row – 191/55)***

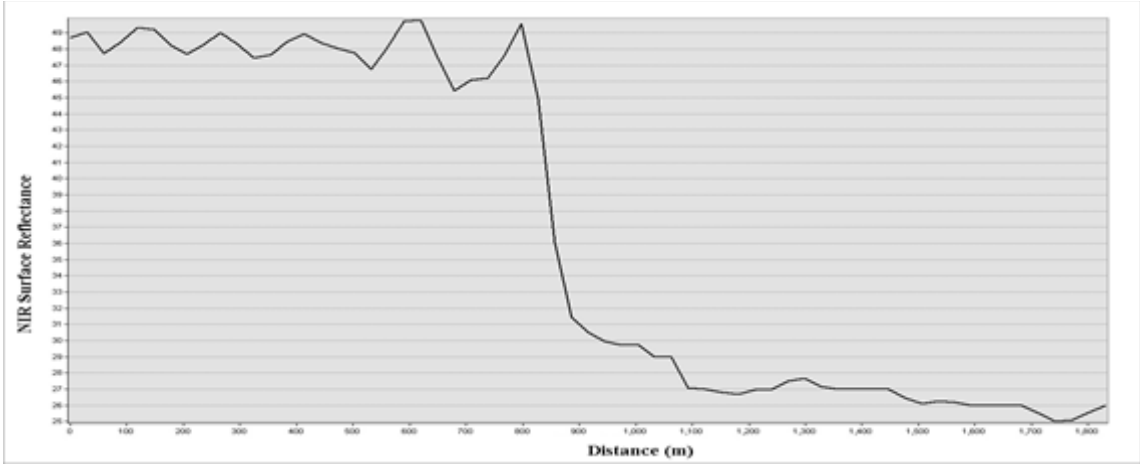

Figure 4: Profile graph for ***Landsat 7 NIR Band 4 – 2006 (Path/Row – 191/55)***

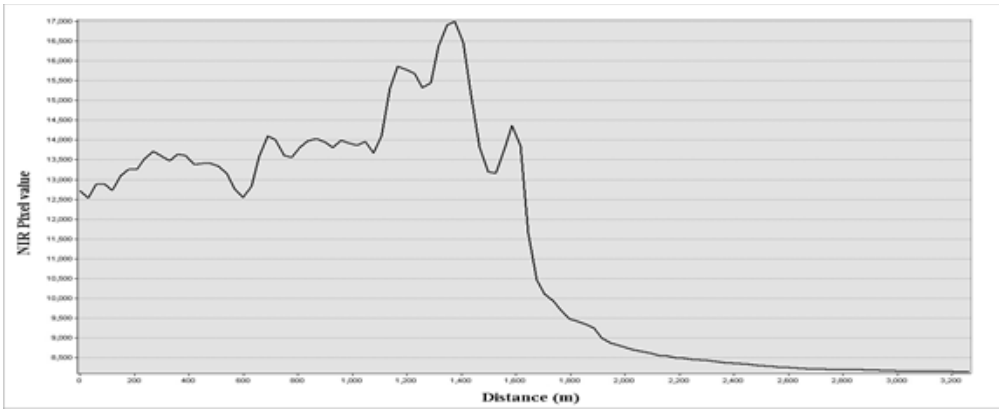

Figure 5: Profile graph for ***Landsat 8 NIR Band 6 – 2015 (Path/Row – 191/55)***

3D visualizations of the creek's bathymetry were generated on Surfer from a surface model created by Inverse Distance Weighted (IDW) interpolation of the depth points. IDW tool uses a method of interpolation that estimates cell values by averaging the values of sample data points in the neighbourhood of each processing cell. The depths were multiplied by a Z-unit conversion factor of -1 to ensure the surface was dropped below datum. To calculate the creek's surface volumes at the 3 epochs on ArcGIS, the IDW surface was converted to a Triangulated Irregular Networks (TIN). Next, the area and volume of the region between the bathymetry surfaces and the reference plane at mean sea level of 0m was calculated from the TIN with the Surface Volume tool. Surface Volume calculates the projected area (2D), surface area (3D), and volume of a surface relative to a given base height, or reference plane. The output results were written to a comma-delimited ASCII text file. Lastly, to visualize the changing depth profile over the 3 epochs, a 2.85km navigation route was designed and a series of depth values were plotted against horizontal distances on GlobalMapper.

3.0 Results

Bathymetric changes in the creek for 1448 sampled points are summarized in Table 3. Maximum depth in 2002 was 9.58m. This reduced to 7.98m in 2006 and 5.50m in 2015. Minimum depth in 2002 was 0.02m. This increased to 0.45m in 2006 and reduced to 0.23m in 2015. The average depth for 2002 was 4.85m. This reduced to 3.76m in 2006 and 3.73m in 2015. Bathymetric charts produced from the Landsat estimations are shown in Figures 6 (a-c). The volumetric calculations presented in Table 4 show that the surface volume was 6,971,566.2m^3 as at December 2002. This reduced to 4,869,175.7m^3 in December 2006 and subsequently increased to 5,094,096.5m^3 in January 2015. In the 4-year period from 2002 – 2006, the decrease in volume was 2,102,390.5m^3. However, in the longer 9-year period from 2006 – 2015, the volume increased by 224,920m^3.

The 3D models of bathymetry for the three epochs are shown in Figure 7. A close visualization shows the 2002 surface is characterized by a series of interconnecting ridges and depressions with some spikes more pronounced at the mid-section of the creek. In 2006, this undulating terrain is less pronounced and the ridges appear to be levelling out gradually. By 2015, most of the surface is fully flattened out and the creek's bottom level has dropped visibly.

Table 3: Change in Lighthouse Creek Bathymetry (2002 – 2015)

Statistic	Depths (m)			Change in Depth (ΔH)	
	2002	2006	2015	$\Delta H_{2015\text{-}2006}$ (m)	$\Delta H_{2006\text{-}2002}$ (m)
Count	1448				
Min	0.02	0.45	0.23	-3.48	-8.05
Max	9.58	7.98	5.50	3.75	4.45
Range	9.55	7.54	5.27	7.24	12.50
Mean	4.85	3.76	3.73	-0.03	-1.08
Std. Dev	2.29	1.55	1.33	1.29	2.07

Table 4: Changes in underwater surface volumes for Lighthouse Creek

	Area 2D (m^2)	Area 3D (m^2)	Volume (m^3)
Dec. 2002	1,283,540.5	1,285,177.6	6,971,566.2
Dec. 2006	1,285,150.0	1,285,986.4	4,869,175.7
Jan. 2015	1,285,900.0	1,286,336.6	5,094,096.5

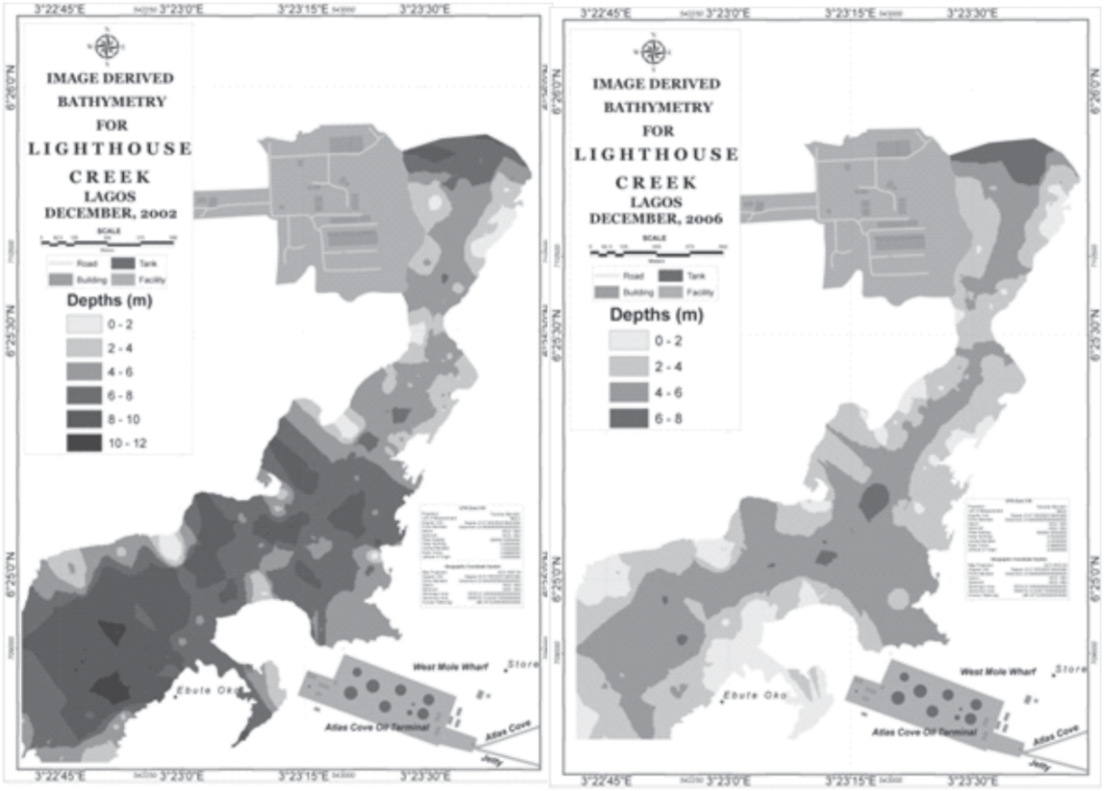

(a) (b)

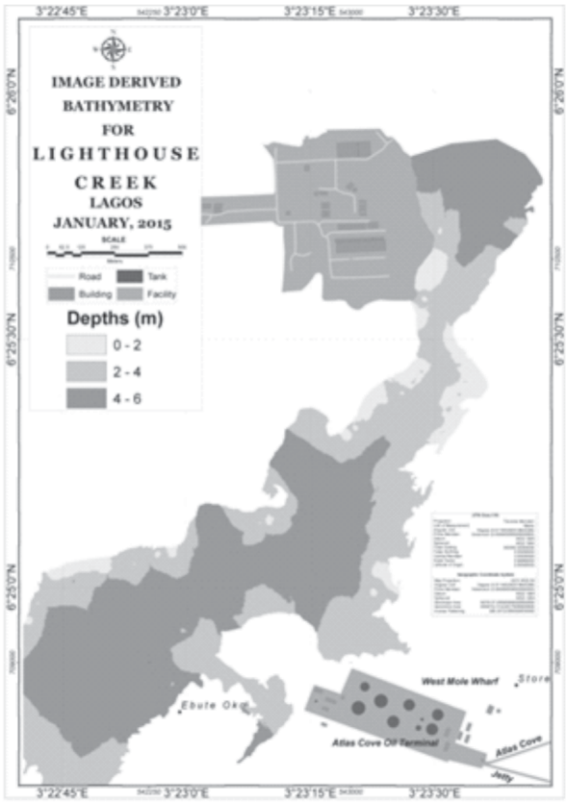

(c)

Figure 6: Landsat derived bathymetry for Lighthouse Creek – (a) 2002 (b) 2006 and (c) 2015

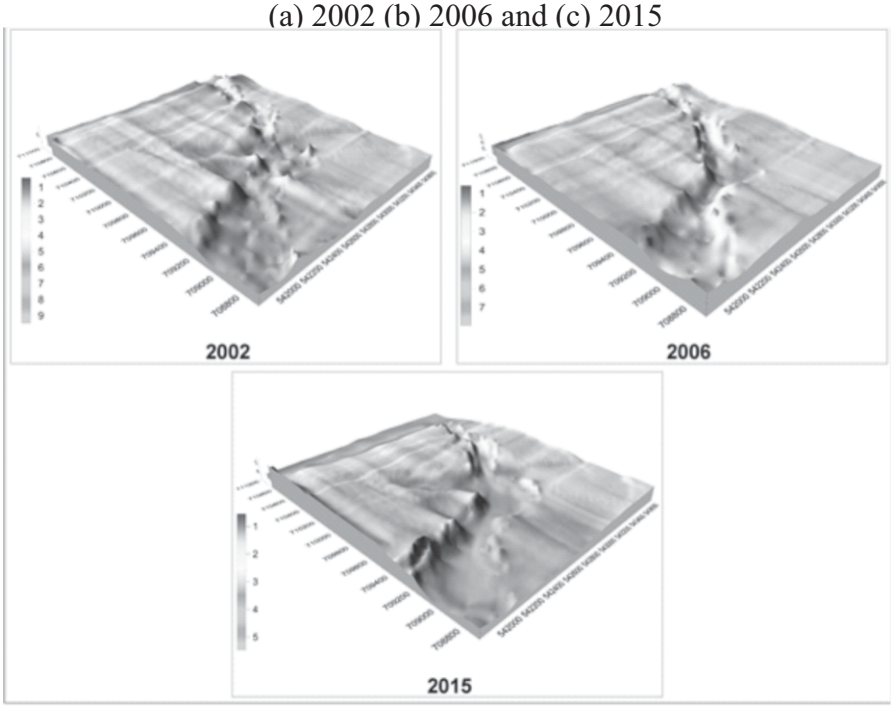

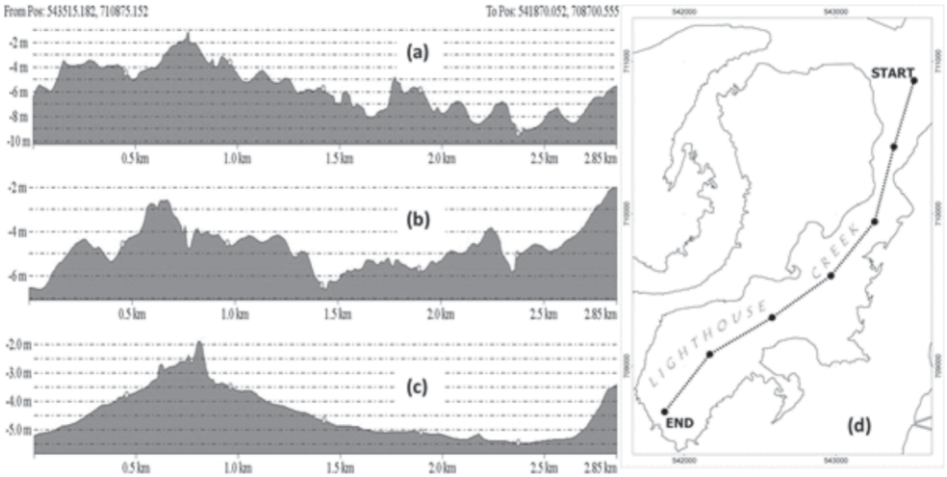

Figure 8: Profiles along designed navigation route –
(a) Dec. 2002 (b) Dec. 2006 and (c) Jan. 2015 (d) Path of profile along creek

Figure 8 shows the longitudinal profile of the 2.85km navigation route designed along the creek with start point at 543515.182*mE*, 710875.152*mN* and endpoint at 541870.052*mE*, 708700.555*mN* (*mE, mN – Easting, Northing*). The profile trend shows a series of rising and falling surfaces as at 2002 with the highest point noticeable between the 0.5 – 1.0km limit. This rippling topography persists until 2015 when it levels out from the highest point into a gently sloping and flat riverbed.

There has also been a rise in construction activity and land reclamation in the creek's vicinity over time, which has impacted on the spatial extent and stability of the underwater structure and ecosystem. In Figure 9, satellite imagery shows the situation of the creek's environment at two epochs (2000 and 2015).

Figure 9: Increased construction activity (circled in red) impacting the Lighthouse creek

4.0 Discussion of Results

From the volumetric estimates, there is an indication that there was an increasing rate of accretion in the Lighthouse Creek until the 2006 period when the seabed material started flowing away gradually from the Creek. It is possible that this flow was in the direction of the Commodore channel to fill up gaps caused by dredging works. The dredging enlarges the cross-section of the channel creating more sediment accommodation space. Aside the contribution of the dredging works in the Commodore channel, the position of the channel at the sediment transition zone between the Lagos Lagoon and the Atlantic Ocean is another factor. This is a zone of sediment transportation caused by the force of water flowing from the Lagos Lagoon into the Atlantic Ocean. This flow upsets the delicate cohesion and compaction of the channel's bed thus causing some of its sediments to be washed away into the ocean. The Commodore channel reacts to the vacuum created by importing sediments to restore its equilibrium. The epochs under study show the general trend of increasing surface volumes with increasing depths and vice versa.

5.0 Conclusion and Recommendations

5.1 Conclusion

This study has investigated changes in the underwater topography of the Lighthouse Creek in Lagos using bathymetric data derived from Landsat imagery. The bathymetry derivation was based on the ratio algorithm developed by Stumpf et al (2003). The volumetric analysis showed a massive build-up of sediments on the creek's bed in the 2002 – 2006 time period. However, in the 2006 – 2015 period, there was mass flow of sediments away from the creek. The reason for this trend could be attributed to the disturbance of the seabed morphology due to dredging and other harbour works in the adjacent Commodore channel. Further investigation is needed to determine the source of the initial sediment build-up and the direction of the present sediment outflow. In conclusion, since the existing bathymetric data for the Lighthouse Creek from previous surveys was spatially incomplete, satellite derived bathymetry offers us a viable solution to study the underwater topography at reasonable scales. Also, the historical archive of the Landsat mission and its frequent revisit time offers added advantages for monitoring such changes over a lengthy time period or since the last hydrographic survey of an area was done. These products can serve as stand-alone information in inaccessible areas or can be used in combination with traditional in-situ data to generate a variety of information layers. More importantly, the Landsat-derived data serves to complement and fill in gaps in the existing bathymetric data coverage for the creek.

5.2 Recommendations

A detailed assessment of the impacts of dredging and other harbour works on the Lighthouse Creek should be done to determine their effects on water flows and sediment fluxes in the adjoining rivers and creeks. An integrated coastal management plan and good coastal management policies are needed to ensure that the stability of this marine ecosystem is maintained. Apart from the presented methodology, nonlinear optimization techniques and other machine learning methods such as Artificial Neural Networks (ANNs) provide an interesting alternative to examine the morphology of

water bodies. Further research is required to improve existing models or to develop more robust models for a more comprehensive characterisation of the underwater terrain.

References

Alsubaie, N.M. (2012). The Potential of Using Worldview-2 Imagery for Shallow Water Depth Mapping. MSc Thesis. UCGE Reports Number 20368. (url: http://www.geomatics.ucalgary.ca/graduatetheses)

Bierwirth, P. N., Lee, T. J., and Burne, R. V. (1993). *Shallow Sea-floor Reflectance and Water depth derived by un-mixing Multispectral Imagery.* Photogrammetric Society and Remote Sensing. 59: 331-338.

Clark, R. K., Fay, T.H., and Walker C.L. (1987). Bathymetry calculations with Landsat 4 TM imagery under a generalized ratio assumption. Applied Optics 26 (19): 4036-4038.

Gao, J. (2009). *Bathymetric mapping by means of remote sensing: methods, accuracy and limitations*. Progress in Physical Geography. 33 (1): 103-116.

Gholamalifard, M., Kutser, T., Esmaili-Sari, A., Abkar, A.A., and Naimi, B. (2013). Remotely Sensed Empirical Modelling of Bathymetry in the Southeastern Caspian Sea. *Remote Sens. 5:* 2746-2762; doi:10.3390/rs5062746

Gordon, H. R., Clark, D.K., Brown, J.W., Brown, O.B. Evans, R.H., and Broenkow, W.W. (1983). Phytoplankton pigment concentrations in the Middle Atlantic Bight: Comparison of ship determinations and CZCS estimates. Appl. Opt. 22: 20-36.

Green, E., Edwards, A., and Mumby, P. (2000). Mapping Bathymetry. In: *Remote sensing handbook for tropical coastal management* (edited by A. J. Edwards), Coastal Management Sourcebook 3, UNESCO Paris, 219-233.

Hedley, J. D., Harborne, A.R. and Mumby, P.J. (2005). Simple and robust removal of sun glint for mapping shallow-water benthos. *International Journal of Remote Sensing.* 26 (10): 2107–2112.

Herban, I.S., and Alionescu, A. (2012). Creating 3d Model and Bathymetric Contour Map using a Modern Topographical Approach. Geocad 2012.

Jawak, S.D., Vadlamani, S.S. and Luis, A.J. (2015). A Synoptic Review on Deriving Bathymetry Information Using Remote Sensing Technologies: Models, Methods and Comparisons. *Advances in Remote Sensing*, 4: 147-162. http://dx.doi.org/10.4236/ars.2015.42013

Lea, D.M., and Legleiter, C.J. (2015). Mapping spatial patterns of stream power and channel change along a gravel-bed river in northern Yellowstone, Geomorphology (2015), http://dx.doi.org/10.1016/j.geomorph.2015.05.033

Liceaga-Correa, M.A., and Euan-Villa, J.I. (2002). Assessment of coral reef bathymetry mapping using visible Landsat Thematic Mapper data. Int. J. Remote Sens. 2002 (23): 3–14.

Lyzenga, D. R. (1985). Shallow-water bathymetry using combined lidar and passive multispectral scanner data. International Journal of Remote Sensing. 6: 115.

Misnan, S.Z. (2011). Bathymetric Mapping from Optical Remotely Sensed Satellite Images. M.Sc. Presentation. University College London.

Nga, L.N., and Nga, N.T.K. (2007). Bathymetry Mapping from Satellite Images for Ly Son Island, Quang Ngai Province. VNU Journal of Science, Earth sciences, T.XXIII, N01, 2007

Olayinka D.N., and Okolie C.J. (2016). Satellite-Derived Bathymetry Modelling in Shallow Water: A Case Study of Lighthouse Creek, Lagos. FIG Working Week 2016, New Zealand, May 2–6, 2016, 16pp. http://www.fig.net/resources/proceedings/fig_proceedings/fig2016/techprog.htm

Onyema, I.C. (2009). Notes on the existence of an additional lagoon in South-western Nigeria: Apẹsẹ Lagoon. Journal of American Science. 5(4): 151-156.

Peeri, S., Azuike, C., Alexander, L., Parrish, C., and Armstrong, A. (2012). Beyond the Chart: the Use of Satellite Remote Sensing for Assessing Chart Adequacy and Completeness Information. CHC 2012 The Arctic, Old Challenges, New Approaches Niagara Falls, Canada 15-17 May 2012.

Pennucci, G., Grasso, R. and Trees, C. (2006). Bathymetry Estimation from High-Resolution Satellite Images. http://geos2.nurc.nato.int/mreaconf/posters/151_Pennucci.pdf

Rodriguez, R.R. (2015). Integration of Topographic and Bathymetric Digital Elevation Model using ArcGIS Interpolation Methods: A Case Study of the Klamath River Estuary. M.Sc. Thesis. University of Southern California.

Stumpf, R. P., Holderied, K., and Sinclair, M. (2003). Determination of water depth with high-resolution satellite imagery over variable bottom types, *Limnology and Oceanography*. 48: 547-556.

Vahtmäe, E., and Kutser, T. (2007). Mapping Bottom type and Water depth in Shallow Coastal Waters with Satellite Remote Sensing. *J. Coast. Res. SI50*: 185–189.

Zirek, E., and Sunar, F. (2014). Change Detection of Seafloor Topography by Modeling Multitemporal Multibeam Echosounder Measurements. The International Archives of the Photogrammetry, Remote Sensing and Spatial Information Sciences, Volume XL-7, 2014. ISPRS Technical Commission VII Symposium, 29 September – 2 October 2014, Istanbul, Turkey